HHS Public Access

Author manuscript

Prostate. Author manuscript; available in PMC 2018 August 10.

Published in final edited form as:

Prostate. 2017 May ; 77(13): 1344–1355. doi:10.1002/pros.23394.

Molecular pathogenesis of human prostate basal cell hyperplasia

Gervaise Henry[1], **Alicia Malewska**[1], **Ryan Mauck**[1], **Jeffrey Gahan**[1], **Ryan Hutchinson**[1], **Jose Torrealba**[2], **Franto Francis**[2], **Claus Roehrborn**[1], and **Douglas Strand**[1,iD]

[1]Department of Urology, UT Southwestern Medical Center, Dallas, Texas

[2]Department of Pathology, UT Southwestern Medical Center, Dallas, Texas

Abstract

Background—Understanding the molecular pathogenesis of distinct phenotypes in human benign prostatic hyperplasia (BPH) is essential to improving therapeutic intervention. Current therapies target smooth muscle and luminal epithelia for relief of lower urinary tract symptoms (LUTS) due to BPH, but basal cell hyperplasia (BCH) remains untargeted. The incidence of has been reported at 8–10%, but a molecular and cellular characterization has not been performed on this phenotype.

Methods—Using freshly digested tissue from surgical specimens, we performed RNA-seq analysis of flow cytometry-purified basal epithelia from 3 patients with and 4 patients without a majority BCH phenotype. qPCR was performed on 28 genes identified as significant from 13 non-BCH and 7 BCH specimens to confirm transcriptomic analysis. IHC was performed on several non-BCH and BCH specimens for 3 proteins identified as significant by transcriptomic analysis.

Results—A total of 141 human BPH specimens were analyzed for the presence of BCH. Clinical characteristics of non-BCH and BCH cohorts revealed no significant differences in age, PSA, prostate volume, medical treatment, or comorbidities. Quantitation of cellular subsets by flow cytometry in 11 BCH patients vs. 11 non-BCH patients demonstrated a significant increase in the ratio of basal to luminal epithelia in patients with BCH ($P < 0.05$), but no significant differences in the total number of leukocytes. RNA-seq data from flow cytometry isolated basal epithelia from patients with and without BCH were subjected to gene set enrichment analysis of differentially expressed genes, which revealed increased expression of members of the epidermal differentiation complex. Transcriptomic data were complemented by immunohistochemistry for members of the epidermal differentiation complex, revealing a morphological similarity to other stratified squamous epithelial layers.

Conclusions—Increased expression of epidermal differentiation complex members and altered epithelial stratification resembles the progression of other metaplastic diseases. These data provide

Correspondence, Douglas Strand, Department of Urology, UT Southwestern Medical Center, 5323 Harry Hines Blvd, Dallas, TX 75390. douglas.strand@UTSouthwestern.edu.

ORCID

Douglas Strand http://orcid.org/0000-0002-0746-927X

CONFLICTS OF INTEREST

The authors declare no relevant conflicts of interest.

insight into the plasticity of the human prostate epithelium and suggest a classification of basal cell hyperplasia as a metaplasia.

Keywords

basal cell hyperplasia; benign prostatic hyperplasia; human prostate; molecular pathogenesis

1 | BACKGROUND

The incidence rate of benign prostatic hyperplasia (BPH) and lower urinary tract symptoms (LUTS) increases approximately 10% per decade of life starting at 40 years of age.[1] Increased life expectancy is associated with increased chronic disease, and the number of people over 80 years old is estimated to increase to 19.5 million in 2030.[2] The number of men in the United States with LUTS is estimated to reach 11 million by 2030.[3] The economic costs of treating LUTS is estimated at more than $4 billion per year.[4] With an increase in specific comorbidities of BPH/LUTS,[5,6] the incidence and progression rates of BPH/LUTS as well as the economic burden are likely to increase.

LUTS due to an enlarged prostate are predominantly treated with 5-alpha reductase inhibitors (5ARI), which reduce total prostate volume ~20% through apoptosis of androgen-dependent luminal epithelia. This medication must be administered continuously with some undesirable side effects.[7] 5ARI treatment only reduces the risk of LUTS progression by 34%, exemplifying the need for personalized therapy.[8] Developing precision medicines will require a deeper understanding the molecular pathogenesis of specific phenotypes.

Although prostate anatomy is variable across mammalian species, its cellular architecture is consistent. Stratified columnar epithelial glands are composed of a squamous basal cell layer and a secretory luminal cell layer that express distinct transcriptomes.[9] The incidence of basal cell hyperplasia (BCH) in the human prostate ranges from 8% to 10% of autopsy specimens and can be distinguished from basal cell carcinoma (BCC) based on nuclear morphology and proliferation index.[10]

The etiology of BCH is unclear. However, the observation that BCH is associated with chronic lymphocytic inflammation could suggest an initiating event.[11] The normal prostate is an immunocompetent organ that contains small numbers of resident T and Blymphocytes.[12] Chronic inflammation is associated with higher prostate volume, higher risk of urinary retention, and higher risk of symptomatic progression,[13–15] leading some to propose that BPH is an autoimmune disease.[16] However, inflamed prostates do not uniformly display BCH. Hormones are also purported to play a role in BCH and are intimately linked to inflammation.[17]BCH has also been suggested to increase in response to androgen deprivation[18] and 5ARI therapy,[19] but it is unclear whether this is a primary response to luminal epithelial apoptosis or a secondary response to inflammation downstream of 5ARI treatment.

To gain a clearer understanding of the cellular and molecular pathogenesis of BCH, we performed RNA sequencing on flow cytometry-purified basal epithelia from patients with and without BCH. These data reveal that BCH glands mimic the histomorphological and

molecular features of stratified squamous keratinocytes with significant upregulation of members of the epidermal differentiation complex. Examination of corresponding tissue blocks revealed no significant differences in either inflammation or proliferation between BPH specimens with or without BCH. These data provide insight into the plasticity of the human prostate epithelium.

2 | METHODS

2.1 | Sample collection

Prostate specimens used in this study were obtained from 141 patients undergoing transurethral resection (TURP) or simple prostatectomy for symptomatic BPH at UT Southwestern Medical Center and Parkland County Hospital from November 2014 to December 2016. Institutional Review Board approval was obtained for medical record review to retrospectively collect clinical and pathological data on each patient. Clinical data and correlations for all patients are listed in Table 1. Clinical data of BCH versus non-BCH cohorts are listed in Table 2.

2.2 | Tissue processing

Fresh tissue samples were transported in ice-cold saline and immediately dissected into portions for (i) flash freezing in liquid nitrogen; (ii) fixation in 10% formalin followed by paraffin embedding; and (iii) an overnight enzymatic digestion into single cells at 37°C using 1.5 μg/mL collagenase type I (Life Technologies), 10 μM ROCK inhibitor Y-27632 (StemRD), 1 nM DHT (Sigma), 1% antibiotic/antimycotic solution (100×, Corning), and 1% Amphotericin B (250 μg/mL, Life Technologies) in HBSS.[17,20]

2.3 | Flow cytometry

Human prostate basal epithelia ($CD45^-/CD31^-/CD326^+/CD49f^{Hi}/CD26^-$), luminal epithelia ($CD45^-/CD31^-/CD326^+/CD49f^{LO}/CD26^+$), stromal cells ($CD45^-/CD31^-/CD326^-$), and leukocytes ($CD45^+/CD31^-/CD326^-$) were analyzed and isolated by fluorescence activated cell sorting (FACS) in the UT Southwestern CRI Flow Cytometry Core as previously published.[17,20] Antibody sources, catalog numbers, and concentrations are listed in Table 3.

2.4 | Immunohistochemistry

Dual immunohistochemistry was performed as described previously.[17] Briefly, sections were dewaxed and rehydrated followed by a 20min block in 3% H_2O_2 in MeOH. Sections were then subjected to antigen retrieval in boiling citrate solution (pH 6) for 20 min. Sections were then blocked in 2.5% horse serum for 20 mins at room temperature. Primary antibodies were diluted in 2.5% horse serum and incubated for 60min at room temperature or overnight at 4°C. ImmPress-AP Anti-Rabbit (Vector labs, MP-5401) and ImmPress HRP Anti-Mouse (Vector labs, MP-7402) ready-to-use secondary antibodies were incubated at room temperature for 30 mins. Alkaline phosphatase activity was developed with the ImmPACT Vector Red alkaline phosphatase substrate (Vector labs, SK-5105) and peroxidase activity was developed with the Immpact DAB Peroxidase substrate (Vector labs, SK-4105). Primary antibody sources and concentrations are listed in Table 3.

2.5 | RNA-seq analysis

Total RNA from 500 K FACS-purified basal cells was extracted using RNEasy micro columns (Qiagen). RNA quantity and quality was tested and processed for RNA-Seq on a HiSeq 1500 Sequencer (Illumina) in the UT Southwestern Genomics and Microarray Core. Sequences (15–20 million) are aligned with HISAT2[21] duplicates are removed using SAMtools[22] and counts are generated using FeatureCount[23] using the annotations from Gencode V20.[24] Genes identified as Globins, rRNAs, and pseudogenes are removed. Differential expression analysis is performed using edgeR,[25] using a FC cutoff of two and adjusted FDR cutoff of 0.05. Gene expression levels for visualization and downstream analysis utilized FPKM values. These were calculated from trimmed reads (Trimmomatic version 0.32)[26] mapped to Ensembl's human reference genome GRCh37 sourced from Illumina's iGenomes project using TopHat (version 2.0.12)[27] with Bowtie2. Mapped reads were filtered using SAMtools (version 0.1.19) to remove those with a quality score MAPQ less than 10. Quality-filtered, mapped reads were then quantified and the FPKM calculations were performed using CuffQuant and CuffNorm of Cufflinks (version 2.2.1),[28,29] respectively. Gene ontology of DEGs was examined using DAVID (version 6.8).[30,31] Gene sets with a Benjamini corrected P-value of 0.05 or less was considered statistically significant. GSEA[32] was assessed on DEGs to the C2 curated gene set from Molecular Signature Database using a FDR of 0.001 or less was considered statistically significant for GSEA analysis. Heatmaps were generated using gplots package (version 3.0.1)[33] in R. Phylogenic trees were generated using ape package (version 4.0)[34] in R. Principal component analysis plots were generated using ggplot2 package (version 2.2.1)[35] in R utilizing principal components calculated with R's prcomp method. R version 2.6.0 was utilized.[36] Correlation plots were made using RPKM values calculated from freshly digested and matching cryopreserved samples. The gene set used was from DEGs calculated from published normCounts ([9], GSE67070), using the package limma (version 3.30.11)[37] filtered by Benjamini adjusted *P*-values of less than 0.05.

2.6 | qPCR analysis

For quantitative real-time PCR (qPCR) 50 mg flash-frozen tissue was ground using a mortar and pestle in liquid nitrogen and RNA was extracted with Trizol (Ambion) from 13 non-BCH and 7 BCH specimens. 500 ng RNA was then reverse transcribed into cDNA using RT^2 First Strand Kit (Qiagen, Valencia, CA). qPCR was performed using IQ SYBR Green Supermix (BioRad, Hercules, CA) and results were analyzed using BioRad CFX manager software. All results were calculated using ΔΔCt analysis and normalized to RPL27 expression. Primer sequences are listed in Table 4.

2.7 | Accession numbers

The RNA-seq data on three bulk basal cell epithelial samples from BPH tissues with basal hyperplasia and four bulk basal cell epithelial samples from BPH tissues without basal hyperplasia were deposited into the GEO database (GSE99824).

3 | RESULTS

3.1 | Basal cell hyperplasia is an expansion of p63^{+}, but not CK5^{+}/14^{+} basal epithelia

BCH was previously detected in 8–10% of a series of prostatectomy specimens.[10] In our biorepository of 141 human BPH specimens (clinical characteristics and correlations of the entire patient biorepository are detailed in Table 1), we were able to detect BCH in 13 specimens, or 9.2% (Figures 1A vs 1E). The prevalence of BCH within each specimen was variable, occupying 10–60% of the total area (reviewed by F.F.). Table 2 compares the clinical characteristics of the 13 patients with BCH and the 128 patients without BCH. These data demonstrate that patients with BCH were not statistically different than non-BCH patients in every clinical characteristic examined, but were more likely to be on a 5ARI (69% vs 47%, respectively) and displayed a trend toward lower PSA levels, though not statistically significant (5.14 vs 6.98 ng/mL, respectively).

To characterize the cellular composition of glands with BCH, we performed dual immunohistochemistry for common markers of basal cell lineage differentiation such as p63 and cytokeratin 14.[38] We discovered that BCH glands either had no CK14^{+} cells, or glands with a single layer of CK14^{+} cells. Intriguingly, compared to normal prostate glands, the stratified layers of cells supra-basal to the CK14^{+} layer were p63^{+}/CK14^{-} (Figures 1B vs 1F). CK5 expression largely overlapped that observed with CK14 (data not shown). Further analysis of the phenotype of supra-basal cells revealed very low AR positivity, suggesting a loss of traditional prostate luminal epithelial differentiation (Figures 1C vs 1G). In this regard, it is noteworthy that circulating PSA levels displayed a trending lower mean in BCH versus non-BCH BPH patients, but this may also be because patients with BCH were more likely to be treated with a 5ARI (69% vs 47%, respectively) (Table 2). Finally, previous reports of BCH showed that proliferation is moderate in BCH glands (1–3%), but significantly higher than in non-BCH glands (0.1%).[10,39,40] We performed dual IHC for Ki67 and CK14, but found that Ki67 immunoreactivity in BCH was no different than non-BCH phenotypes (Figures 1G vs 1H).

3.2 | FACS analysis of primary human BPH tissues confirms expansion of CD49f^{Hi} basal epithelia in patients with BCH

The ratio of basal to luminal epithelia in normal human prostate glands is around 1:1 by histological examination.[41] To compare the ratio of basal to luminal cells in BCH versusn on-BCH, we used a novel tissue phenotyping approach by multicolor flow cytometry. Previous reports identified high expression of cell surface protein CD49f cell as a marker of basal epithelia[42] and CD26 as a marker of luminal epithelia.[43] It is expensive and logistically difficult to prospectively sort out every cell type from each fresh tissue before the histological phenotype is determined, especially a phenotype such as BCH with an incidence below 10%. We therefore adopted the method of cryopreserving single cell aliquots while the embedding of intact tissue is completed for histological evaluation by a pathologist. Once histology is reviewed, cryopreserved cells are thawed for single cell type analysis and bulk purification by flow cytometry (Figure 2A). We performed an initial bulk sequencing experiment of basal and luminal epithelia sorted from fresh tissue versus cells that were sorted after cryopreservation for 3 months. Plots of fresh versus cryopreserved

basal epithelia and fresh versus cryopreserved luminal epithelia demonstrate strong correlations between fresh and cryopreserved individual cell types from the same patient (Figure 2B). This held true across the whole genome and became even stronger when we specifically looked at a list of basal or luminal cell type-specific genes generated previously by RNA sequencing (targeted genome). Furthermore, a list of differentially expressed genes (DEGs) generated from basal and luminal cells sorted after cryopreservation demonstrated very strong normalized enrichment scores when compared by gene set enrichment analysis (GSEA) to the DEGs of basal and luminal epithelia generated by the Tang lab (Figure 2C).[9] These data provided confidence that the basal epithelial cell transcriptomes generated from cryopreserved cells in our BCH patients display high fidelity to the transcriptome of cells before cryopreservation.

It should be noted that the viability of freshly digested cells versus short- (1 week) or long-term (1 year) cryopreserved aliquots is remarkably similar (~40–50%), but luminal cells are more sensitive to tissue digestion than other cell types (~30% viability for luminal cells, ~60% for basal cells, ~90% for leukocytes, and ~75% for stroma).[20] This means that only a relative ratio of cell types can be inferred from digested tissue.

One issue with single cell type analyses is the inability to examine a tissue's histological architecture before it is enzymatically digested. The advantage of our study is that most of our biospecimens are large simple prostatectomies that maintain tissue contiguity (unlike the chips of tissue generated by TURP of the prostate, or TURP). Therefore, we could identify patients with a majority BCH phenotype and take portions of the same specimen for both digestion and paraffin embedding although it is still not guaranteed that the phenotypes are exactly the same in the embedded portion and the digested portion.

Multicolor flow cytometry allows for an estimate of the ratios of major cell populations to confirm whether the digested portion of the tissue is similar to the embedded portion. First, a viability dye and CD31 are used in the same channel (V450) to simultaneously remove dead cells and endothelia, respectively. We then separate the cells into major lineages including leukocytes ($CD45^+/CD326^-$), epithelia ($CD45^-/CD326^+$), and stroma ($CD45^-/CD326^-$). Epithelia are further subdivided in basal ($CD49f^{HI}/CD26^-$) and luminal ($CD49f^{LO}/CD26^+$) subtypes. Figure 2D demonstrates that the ratio of basal to luminal cells is significantly higher in tissue with BCH compared to non-BCH tissue, adding confidence to our estimation of BCH by pathology. We were able to show a statistically significant increase in percent basal epithelia across 21 samples (10 BCH, 11 non-BCH). Importantly, total $CD45^+$ leukocytes were not significantly different between the two groups (Figure 2E).

3.3 | RNAseq analysis of FACS-purified basal epithelia reveals conversion to a keratinocyte phenotype

The cellular composition of prostate tissue is extremely diverse and focal. Most prostates contain multiple glandular and stromal phenotypes adjacent to each other, which leads to an averaging of the molecular signal of specific phenotypes if the whole tissue is ground up for analysis. In order to generate a clean molecular profile of BCH, free of contaminating signal from leukocytes, stroma, and luminal epithelia, we performed RNA sequencing on bulk-isolated basal epithelia from three patients with basal hyperplasia and four patients without

BCH per our previous protocol.[20] A dendrogram of unsupervised reads revealed a significant clustering of BCH and non- BCH transcriptomes (Figure 3A), which was confirmed with principal component analysis shown by heat map in Figure 3B. DAVID analysis[44] revealed several biological pathways related to epidermis and keratinocyte differentiation (Figure 3C). GSEA[32] identified several significantly similar DEG sets, with the highest enrichment of an epithelial differentiation module (Figure 3D). The enrichment of a curated set of epidermal differentiation complex genes listed in Figure 3E indicated a potential keratinocyte conversion, which we proceeded to confirm by qPCR.

3.4 | qPCR confirmation of epidermal differentiation complex gene expression in BCH

Barrier tissues such as the epidermis and esophagus are a stratified epithelium composed of several layers. Basal keratinocytes expressing KRT5/14 (stratum basale) commit to epidermal differentiation by exit from the cell cycle and a supra-basal migration to the spinous, granular, and cornified layers. Each layer is characterized by the expression of genes such as transglutaminases, keratins, cornified envelope precursors, the S100A proteins, and the S100 fused type proteins, which are collectively referred to as the epidermal differentiation complex.[45] In order to confirm the potential for an enrichment of epidermal differentiation complex genes in BCH (Figure 3E), we performed qPCR on pieces of whole tissue from 7 patients with BCH and 13 patients without BCH. This was done because limited amounts of RNA can be extracted from sorted cells, and this was used for sequencing. Results show that several of the top differentially expressed epidermal differentiation complex genes were significantly increased in BCH tissues (Figure 4A–F). We first examined the expression of several known prostate lineage-specific differentiation markers, which showed a decrease in AR and PSA in BCH specimens as expected (Figure 4A). We then systematically examined expression of epidermal differentiation complex genes including keratinocyte keratins (Figure 4B), members of the cornified envelope protein (CEP) family (Figure 4C), the S100 fused type protein (SFTP) family (Figure 4D), the S100A family, and various other keratinocyte markers selected from the significant EDC DEGs shown in Figures 3E and 4E.

3.5 | IHC analysis confirms keratinocyte differentiation in BCH

BCH is a focal phenotype that can occupy any where from 10% to 60% of the total transition zone. We performed immunohistochemistry (IHC) to confirm the RNA sequencing and qPCR results. First, to rule out the potential for adenocarcinoma, which can sometimes show p63 positivity, we performed IHC with a p40 antibody instead of p63 (Figure 5A–D). Dual staining of p40 with CK14 demonstrated similar results to that observed with p63, confirming the lack of adenocarcinoma. We then performed dual IHC for CK14 and cornulin (CRNN), one of the EDC genes significantly upregulated in our sequencing and qPCR data. Figure 5E–H demonstrates the complete lack of CRNN reactivity in non-BCH tissue while supra-basal, CK14−/p63+ cells showed focal reactivity for CRNN. Finally, cytokeratin 10 (CK10) is another marker commonly increased in squamous metaplasia and upregulated in our sequencing and qPCR data (Figures 3E and 4B) that was differentially expressed in BCH versus non-BCH tissues (Figure 5I–L).

4 | DISCUSSION

We present a novel approach to characterizing the molecular pathogenesis of a unique BPH phenotype. BPH is an umbrella term that includes a wide range of pathologies including BCH, stromal cell hyperplasia, and glandular hyperplasia.[46] Prostatic basal cell proliferation can range from ordinary BCH to florid BCH and basal cell carcinoma (BCC). Our fresh tissue biorepository specimens did not contain either florid BCH or BCC. The reported incidence of BCH ranges from 8% to 10%[10].We report here the incidence of BCH in our cohort of 141 BPH patients at 9.2%. Moreover, patients with BCH also display lower local and circulating PSA levels (Figure 4A and Table 2).

A metaplastic differentiation event is commonly observed in response to chronic injury or inflammation such as in Barrett's esophagus where the normal stratified squamous epithelium of the esophagus changes into a columnar epithelium with features of stomach and intestine.[47] In fact, in our DAVID analysis of BCH transcriptomes, the top related tissues were esophagus, keratinocyte, and tongue (data not shown). It has been suggested that BCH is a precursor lesion to BCC given that extensive BCH is observed in patients with BCC.[48–51] Similar to the links between BCH and BCC, Barrett's esophagus is thought to be a precursor lesion for esophageal cancer. However, the initiating events and the cell of origin (reprogrammed stem cell vs transdifferentiation of terminal cells) are still debated in Barrett's esophagus.[52,53] Likewise, our understanding of the etiology and pathogenesis of prostatic BCH is unclear.

The association between LUTS progression and chronic infiltration is well-documented.[13,54–56] Chronic inflammation is associated with higher prostate volume, higher risk of urinary retention, and higher risk of symptomatic progression in the MTOPS and REDUCE trials.[13,57] The identification of resident and infiltrating T cells in the prostate has revealed the potential autoimmune nature of BPH,[12,58–60] but the molecular links underlying the causes and responses to inflammation are poorly understood.[61,62] We did not detect a significant difference in the total number of leukocytes between BPH with BCH versus BPH without BCH (Figure 2E). Moreover, it is unclear why the prostate can display high levels of inflammation without BCH if this is a putative initiation event. There is also the possibility that a change in the balance of androgens and estrogens can drive BCH,[18,19] independent of hormonal effects on inflammation. Sixty-nine percent of our patients with BCH were on 5ARI treatment, but so were 49% of patients in the non-BCH cohort (Table 2), suggesting the phenotype is not strictly treatment-induced. However, we did not measure circulating or local tissue levels of androgens or estrogens, which in the future could help explain the potential role of hormones in the etiology of BCH.

In summary, our data demonstrate a conversion of the single cell layer of $CK5^{+}/CK14^{+}/p63^{+}/p40^{-}/CK10^{-}$ basal epithelia to a stratified squamous epithelium resembling keratinocytes of the skin, tongue, and esophagus (Figure 6). It is likely that the lack of luminal epithelia in the prostate glands of patients with BCH will render these patients insensitive to the reduction in prostate volume elicited with 5ARI treatment. This is a prime example of the need for personalized treatment options for clinicians to treat BPH based on prostate pathology rather than clinical data such as prostate volume and PSA levels. This

will require the development of biomarkers or high-resolution imaging techniques capable of diagnosing BPH pathology in the clinic.

Acknowledgments

Research reported in this publication was supported by the National Center for Advancing Translational Sciences of the National Institutes of Health under award number UL1TR001105. The content is solely the responsibility of the authors and does not necessarily represent the official views of the NIH.

Funding information

National Institute of Diabetes and Digestive and Kidney Diseases, Grant numbers: 1K01DK098277, 1R03DK110497; National Center for Advancing Translational Sciences of the National Institutes of Health, Grant number: UL1TR001105

References

1. Platz EA, Joshu CE, Mondul AM, Peskoe SB, Willett WC, Giovannucci E. Incidence and progression of lower urinary tract symptoms in a large prospective cohort of United States men. J Urol. 2012; 188:496–501. [PubMed: 22704110]
2. CDC. The State of Aging and Health in America. 2013 2013.
3. Jacobsen SJ, Girman CJ, Guess HA, Oesterling JE, Lieber MM. New diagnostic and treatment guidelines for benign prostatic hyperplasia. Potential impact in the United States. Arch Intern Med. 1995; 155:477–481. [PubMed: 7532392]
4. Saigal CS, Joyce G. Economic costs of benign prostatic hyperplasia in the private sector. J Urol. 2005; 173:1309–1313. [PubMed: 15758787]
5. Parsons JK, Carter HB, Partin AW, et al. Metabolic factors associated with benign prostatic hyperplasia. J Clin Endocrinol Metab. 2006; 91:2562–2568. [PubMed: 16608892]
6. Mozumdar A, Liguori G. Persistent increase of prevalence of metabolic syndrome among U.S. adults: NHANES III to NHANES 1999–2006. Diabetes Care. 2011; 34:216–219. [PubMed: 20889854]
7. Group TFS. Finasteride (MK-906) in the treatment of benign prostatic hyperplasia. The Finasteride Study Group. Prostate. 1993; 22:291–299. [PubMed: 7684524]
8. Bechis SK, Otsetov AG, Ge R, Olumi AF. Personalized medicine for the management of benign prostatic hyperplasia. J Urol. 2014; 192:16–23. [PubMed: 24582540]
9. Zhang D, Park D, Zhong Y, et al. Stem cell and neurogenic gene-expression profiles link prostate basal cells to aggressive prostate cancer. Nat Commun. 2016; 7:10798. [PubMed: 26924072]
10. Thorson P, Swanson PE, Vollmer RT, Humphrey PA. Basal cell hyperplasia in the peripheral zone of the prostate. Mod Pathol. 2003; 16:598–606. [PubMed: 12808066]
11. Devaraj LT, Bostwick DG. Atypical basal cell hyperplasia of the prostate. Immunophenotypic profile and proposed classification of basal cell proliferations. Am J Surg Pathol. 1993; 17:645–659. [PubMed: 7686348]
12. Steiner G, Gessl A, Kramer G, Schollhammer A, Forster O, Marberger M. Phenotype and function of peripheral and prostatic lymphocytes in patients with benign prostatic hyperplasia. J Urol. 1994; 151:480–484. [PubMed: 7506795]
13. Nickel JC, Roehrborn CG, O'Leary MP, Bostwick DG, Somerville MC, Rittmaster RS. The relationship between prostate inflammation and lower urinary tract symptoms: examination of baseline data from the REDUCE trial. Eur Urol. 2008; 54:1379–1384. [PubMed: 18036719]
14. Di Silverio F, Gentile V, De Matteis A, et al. Distribution of inflammation, pre-malignant lesions, incidental carcinoma in histologically confirmed benign prostatic hyperplasia: a retrospective analysis. Eur Urol. 2003; 43:164–175. [PubMed: 12565775]
15. Roehrborn CGKS, Noble WD, Slawin KM, McVary KT, Kusek JW. The impact of acute or chronic inflammation in baseline biopsy on the risk of progression in the MTOPS study. Eur Urol Suppl. 2005; 4 Abstract 10.

16. Kramer G, Mitteregger D, Marberger M. Is benign prostatic hyperplasia (BPH) an immune inflammatory disease? Eur Urol. 2007; 51:1202–1216. [PubMed: 17182170]
17. Zhang B, Kwon OJ, Henry G, et al. Non-Cell-Autonomous regulation of prostate epithelial homeostasis by androgen receptor. Mol Cell. 2016
18. Kruithof-Dekker IG, Tetu B, Janssen PJ, Van der Kwast TH. Elevated estrogen receptor expression in human prostatic stromal cells by androgen ablation therapy. J Urol. 1996; 156:1194–1197. [PubMed: 8709345]
19. Bauman TM, Sehgal PD, Johnson KA, et al. Finasteride treatment alters tissue specific androgen receptor expression in prostate tissues. Prostate. 2014; 74:923–932. [PubMed: 24789081]
20. Strand DW, Aaron L, Henry G, Franco OE, Hayward SW. Isolation and analysis of discreet human prostate cellular populations. Differentiation. 2015
21. Kim D, Langmead B, Salzberg SL. HISAT: a fast spliced aligner with low memory requirements. Nat Methods. 2015; 12:357–360. [PubMed: 25751142]
22. Li H, Handsaker B, Wysoker A, et al. Project data processing, the sequence Alignment/Map format and SAMtools. Bioinformatics. 2009; 25:2078–2079. [PubMed: 19505943]
23. Liao Y, Smyth GK, Shi W. FeatureCounts: an efficient general purpose program for assigning sequence reads to genomic features. Bioinformatics. 2014; 30:923–930. [PubMed: 24227677]
24. Harrow J, Frankish A, Gonzalez JM, et al. GENCODE: the reference human genome annotation for The ENCODE Project. Genome Res. 2012; 22:1760–1774. [PubMed: 22955987]
25. Robinson MD, McCarthy DJ, Smyth GK. EdgeR: a Bioconductor package for differential expression analysis of digital gene expression data. Bioinformatics. 2010; 26:139–140. [PubMed: 19910308]
26. Bolger AM, Lohse M, Usadel B. Trimmomatic: a flexible trimmer for Illumina sequence data. Bioinformatics. 2014; 30:2114–2120. [PubMed: 24695404]
27. Kim D, Pertea G, Trapnell C, Pimentel H, Kelley R, Salzberg SL. TopHat2: accurate alignment of transcriptomes in the presence of insertions, deletions and gene fusions. Genome Biol. 2013; 14:R36. [PubMed: 23618408]
28. Roberts A, Trapnell C, Donaghey J, Rinn JL, Pachter L. Improving RNA-Seq expression estimates by correcting for fragment bias. Genome Biol. 2011; 12:R22. [PubMed: 21410973]
29. Trapnell C, Williams BA, Pertea G, et al. Transcript assembly and quantification by RNA-Seq reveals unannotated transcripts and isoform switching during cell differentiation. Nat Biotechnol. 2010; 28:511–515. [PubMed: 20436464]
30. Huang DW, Sherman BT, Lempicki RA. Systematic and integrative analysis of large gene lists using DAVID bioinformatics resources. Nat Protocols. 2009; 4:44–57. [PubMed: 19131956]
31. Huang DW, Sherman BT, Lempicki RA. Bioinformatics enrichment tools: paths toward the comprehensive functional analysis of large gene lists. Nucleic Acids Res. 2009; 37:1–13. [PubMed: 19033363]
32. Subramanian A, Tamayo P, Mootha VK, et al. Gene set enrichment analysis: a knowledge-based approach for interpreting genome-wide expression profiles. Proc Natl Acad Sci USA. 2005; 102:15545–15550. [PubMed: 16199517]
33. Warnes GR, Bolker B, Bonebakker L, et al. gplots: various R Programming Tools for Plotting Data. 2016
34. Paradis E, Claude J, Strimmer K. APE: analyses of phylogenetics and evolution in R language. Bioinformatics. 2004; 20:289–290. [PubMed: 14734327]
35. Wickham, H. ggplot2: Elegant Graphics for Data Analysis. New York: Springer-Verlag; 2009.
36. Team RC. R: A Language and Environment for Statistical Computing. Vienna, Austria: 2016.
37. Ritchie ME, Phipson B, Wu D, et al. Limma powers differential expression analyses for RNA-sequencing and microarray studies. Nucleic Acids Res. 2015; 43:e47. [PubMed: 25605792]
38. Hudson DL, Guy AT, Fry P, O'Hare MJ, Watt FM, Masters JR. Epithelial cell differentiation pathways in the human prostate: identification of intermediate phenotypes by keratin expression. J Histochem Cytochem. 2001; 49:271–278. [PubMed: 11156695]
39. Montironi R, Galluzzi CM, Diamanti L, Giannulis I, Pisani E, Scarpelli M. Prostatic intra-epithelial neoplasia: expression and location of proliferating cell nuclear antigen in epithelial,

endothelial and stromal nuclei. Virchows Arch A Pathol Anat Histopathol. 1993; 422:185–192. [PubMed: 7684168]

40. Kyprianou N, Tu H, Jacobs SC. Apoptotic versus proliferative activities in human benign prostatic hyperplasia. Hum Pathol. 1996; 27:668–675. [PubMed: 8698310]
41. El-Alfy M, Pelletier G, Hermo LS, Labrie F. Unique features of the basal cells of human prostate epithelium. Microsc Res Tech. 2000; 51:436–446. [PubMed: 11074614]
42. Goldstein AS, Lawson DA, Cheng D, Sun W, Garraway IP, Witte ON. Trop2 identifies a subpopulation of murine and human prostate basal cells with stem cell characteristics. Proc Natl Acad Sci USA. 2008; 105:20882–20887. [PubMed: 19088204]
43. Stoyanova T, Cooper AR, Drake JM, et al. Prostate cancer originating in basal cells progresses to adenocarcinoma propagated by luminallike cells. Proc Natl Acad Sci USA. 2013; 110:20111–20116. [PubMed: 24282295]
44. Huang da W, Sherman BT, Lempicki RA. Systematic and integrative analysis of large gene lists using DAVID bioinformatics resources. Nat Protoc. 2009; 4:44–57. [PubMed: 19131956]
45. Candi E, Schmidt R, Melino G. The cornified envelope: A model of cell death in the skin. Nat Rev Mol Cell Biol. 2005; 6:328–340. [PubMed: 15803139]
46. Roehrborn CG. Pathology of benign prostatic hyperplasia. Int J Impot Res. 2008; 20:S11–S18.
47. Naini BV, Souza RF, Odze RD. Barrett's esophagus: a comprehensive and contemporary review for pathologists. AmJ Surg Pathol. 2016; 40:e45–e66. [PubMed: 26813745]
48. Epstein JI, Armas OA. Atypical basal cell hyperplasia of the prostate. Am J Surg Pathol. 1992; 16:1205–1214. [PubMed: 1281386]
49. Mastropasqua MG, Pruneri G, Renne G, De Cobelli O, Viale G. Basaloid cell carcinoma of the prostate. Virchows Arch. 2003; 443:787–791. [PubMed: 14756145]
50. Grignon DJ, Ro JY, Ordonez NG, Ayala AG, Cleary KR. Basal cell hyperplasia, adenoid basal cell tumor, and adenoid cystic carcinoma of the prostate gland: an immunohistochemical study. Hum Pathol. 1988; 19:1425–1433. [PubMed: 2461340]
51. Denholm SW, Webb JN, Howard GC, Chisholm GD. Basaloid carcinoma of the prostate gland: Histogenesis and review of the literature. Histopathology. 1992; 20:151–155. [PubMed: 1559669]
52. Wang X, Ouyang H, Yamamoto Y, et al. Residual embryonic cells as precursors of a barrett's-like metaplasia. Cell. 2011; 145:1023–1035. [PubMed: 21703447]
53. Stairs DB, Nakagawa H, Klein-Szanto A, et al. Cdx1 and c-Myc foster the initiation of transdifferentiation of the normal esophageal squamous epithelium toward Barrett's esophagus. PLoS ONE. 2008; 3:e3534. [PubMed: 18953412]
54. McConnell JD, Roehrborn CG, Bautista OM, et al. Therapy of Prostatic Symptoms Research, The long-term effect of doxazosin, finasteride, and combination therapy on the clinical progression of benign prostatic hyperplasia. N Engl J Med. 2003; 349:2387–2398. [PubMed: 14681504]
55. St Sauver JL, Sarma AV, Jacobson DJ, et al. Associations between C-reactive protein and benign prostatic hyperplasia/lower urinary tract symptom outcomes in a population-based cohort. Am J Epidemiol. 2009; 169:1281–1290. [PubMed: 19395697]
56. Rohrmann S, De Marzo AM, Smit E, Giovannucci E, Platz EA. Serum C-reactive protein concentration and lower urinary tract symptoms in older men in the Third National Health and Nutrition Examination Survey (NHANES III). Prostate. 2005; 62:27–33. [PubMed: 15389816]
57. McConnell JD, Roehrborn CG, Bautista OM, et al. The long-term effect of doxazosin, finasteride, and combination therapy on the clinical progression of benign prostatic hyperplasia. N Engl J Med. 2003; 349:2387–2398. [PubMed: 14681504]
58. Robert G, Descazeaud A, Nicolaiew N, et al. Inflammation in benign prostatic hyperplasia: a 282 patients' immunohistochemical analysis. Prostate. 2009; 69:1774–1780. [PubMed: 19670242]
59. Theyer G, Kramer G, Assmann I, et al. Phenotypic characterization of infiltrating leukocytes in benign prostatic hyperplasia. Lab Invest. 1992; 66:96–107. [PubMed: 1370561]
60. Steiner GE, Stix U, Handisurya A, et al. Cytokine expression pattern in benign prostatic hyperplasia infiltrating T cells and impact of lymphocytic infiltration on cytokine mRNA profile in prostatic tissue. Lab Invest. 2003; 83:1131–1146. [PubMed: 12920242]

61. Steiner GE, Djavan B, Kramer G, et al. The picture of the prostatic lymphokine network is becoming increasingly complex. Rev Urol. 2002; 4:171–177. [PubMed: 16985676]

62. Kwon OJ, Zhang L, Ittmann MM, Xin L. Prostatic inflammation enhances basal-to-luminal differentiation and accelerates initiation of prostate cancer with a basal cell origin. Proc Natl Acad Sci USA. 2014; 111:E592–E600. [PubMed: 24367088]

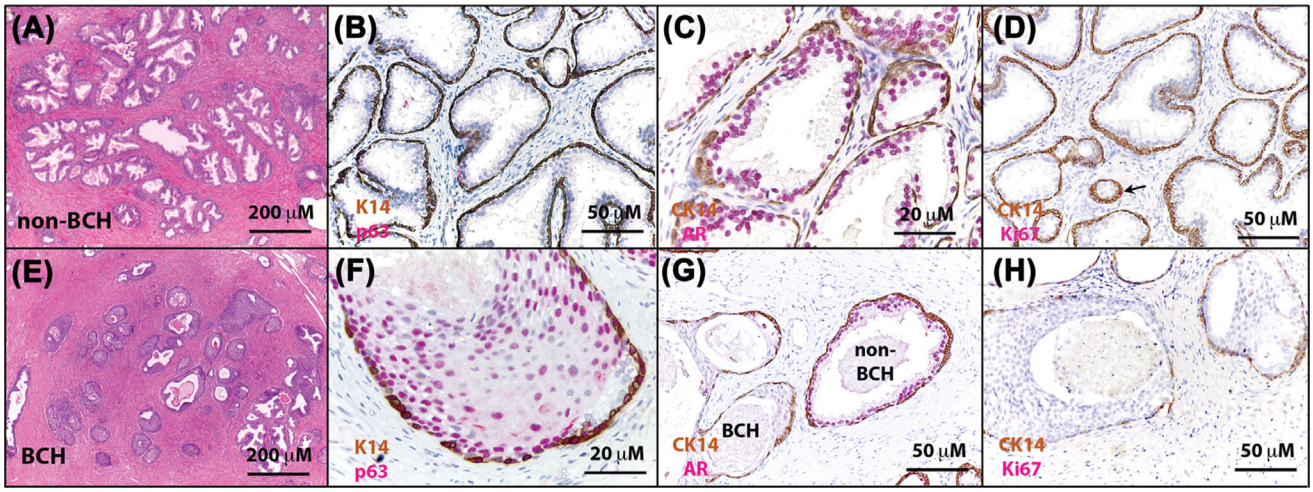

FIGURE 1.

Histological characterization of basal cell hyperplasia. (A and E) Representative H&E stained sections from BPH patient specimens with no BCH and with majority BCH. (B and F) Dual staining with cytokeratin 14 (K14, brown) and p63 (red) shows co-stained basal epithelia in specimens with no BCH, but the emergence of $K14^{-}/p63^{+}$ layers in patients with BCH. (C and G) Dual staining with K14 (brown) and androgen receptor (AR, red) shows loss of luminal cell AR in glands with a BCH phenotype. (D and H) Dual staining with K14 (brown) and Ki67 (red) show rare $K14^{+}$ basal epithelia proliferating in non-BCH phenotypes (arrow) with no increase observed in BCH

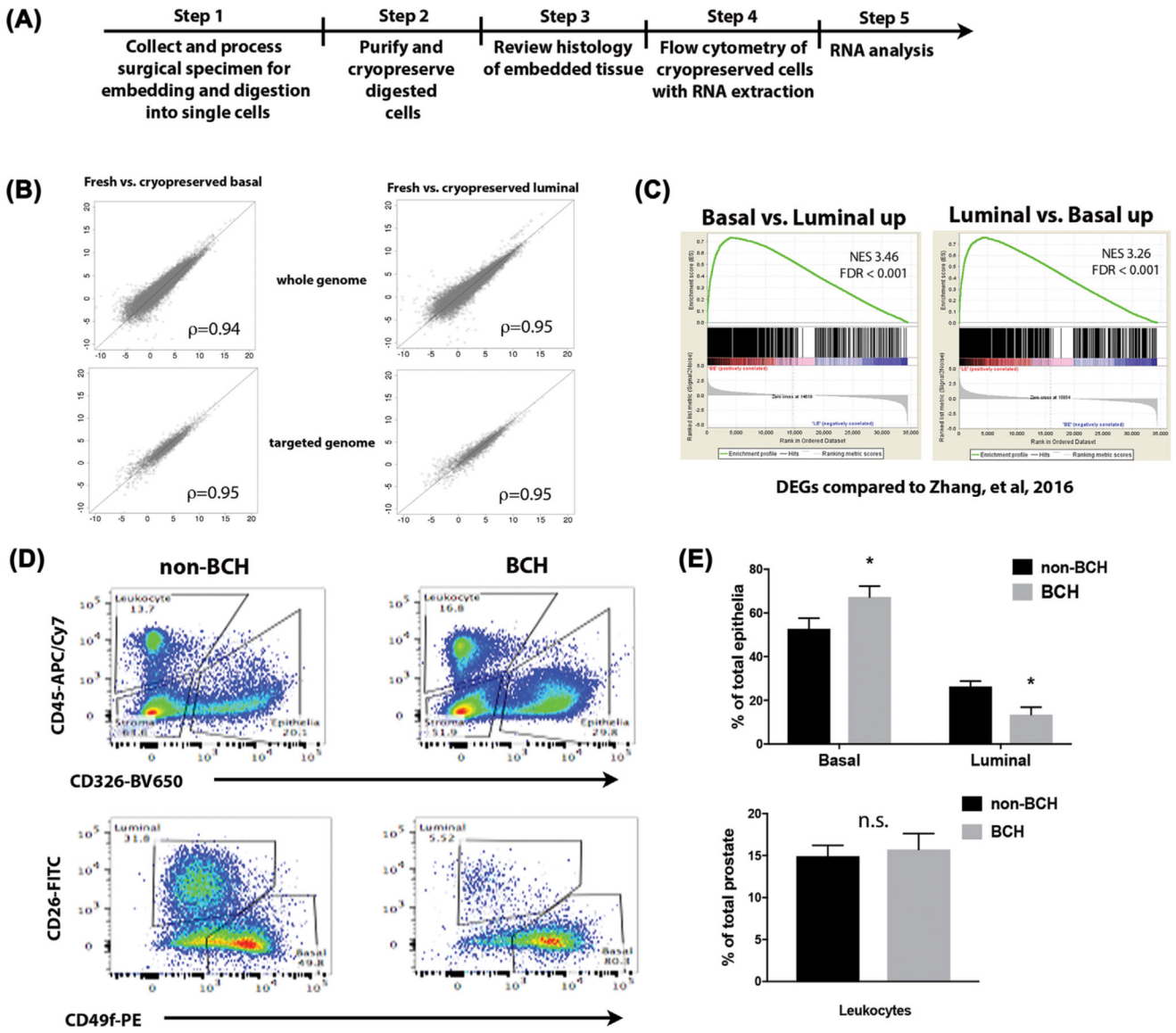

FIGURE 2.

Workflow for transcriptomic analysis of BCH. (A) Stepwise workflow of BPH specimen processing. (B) Correlation analysis of transcriptomes from 1 patient produced from freshly isolated basal and luminal epithelia versus those that were cryopreserved before cDNA library production. (C) Gene set enrichment analysis (GSEA) of differentially expressed genes (DEGs) in cryopreserved basal and luminal epithelia demonstrate data that are highly correlated with basal and luminal transcriptomes generated by Nat Commun, 2016;7:10798. (D) Representative flow cytometry plots from patients with and without BCH. (E) Quantitation of percentages of basal and luminal epithelia from 11 patients with BCH and 11 patients without BCH demonstrates a significant increase in basal epithelia in patients with BCH. There was no significant difference in the number of leukocytes between patients with and without BCH

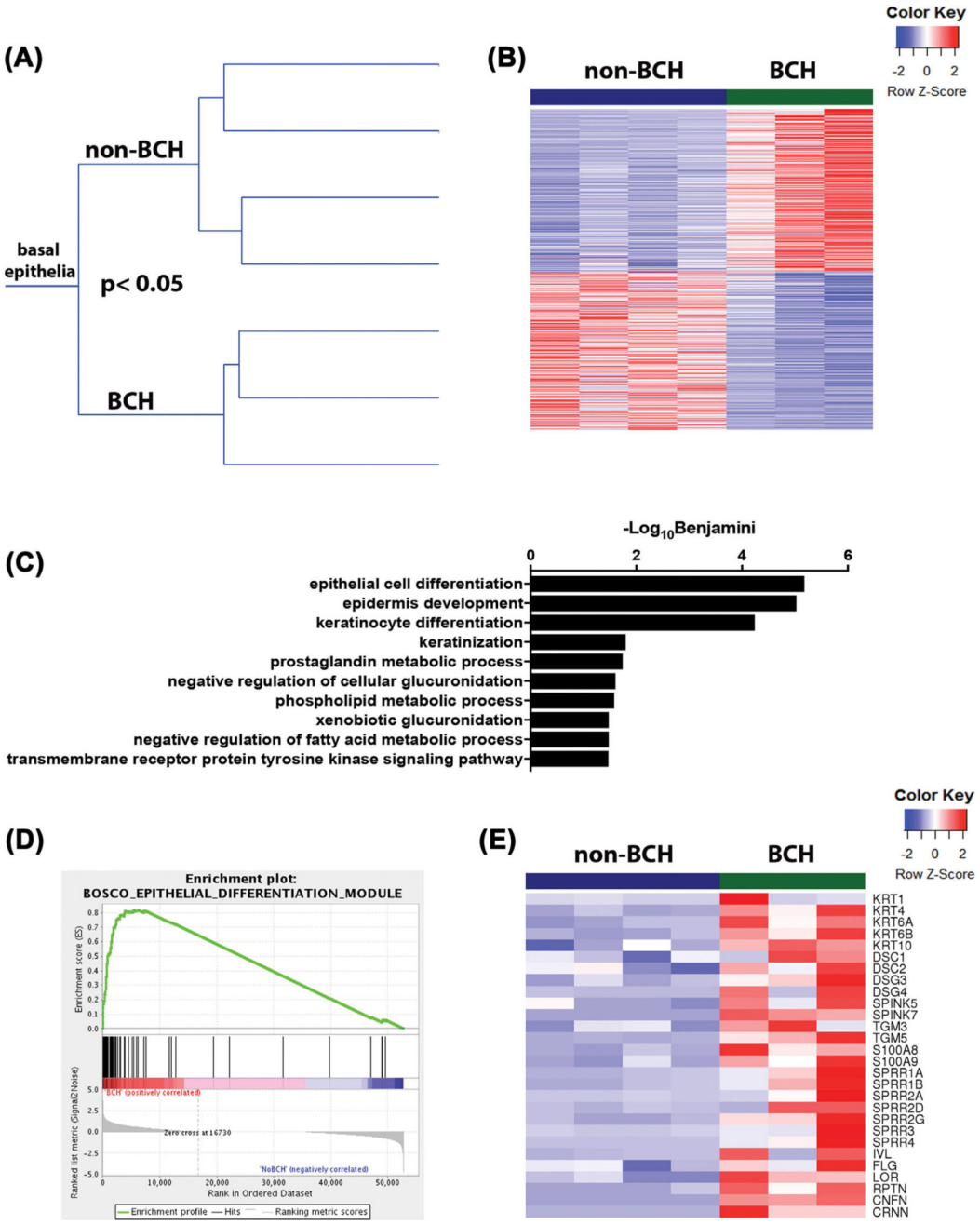

FIGURE 3.

Transcriptomic analysis of basal epithelia from patients with BCH. (A) Dendrogram of unsupervised hierarchical clustering of BCH and non-BCH specimens. (B) Heat map of RNA-sequencing data from BCH and non-BCH specimens. (C) DAVID analysis of transcriptomic data reveals top gene sets matching BCH DEGs. (D) GSEA enrichment plot of BCH genes in the Bosco Epithelial differentiation module. (E) Top 28 genes enriched in BCH related to keratinocyte differentiation

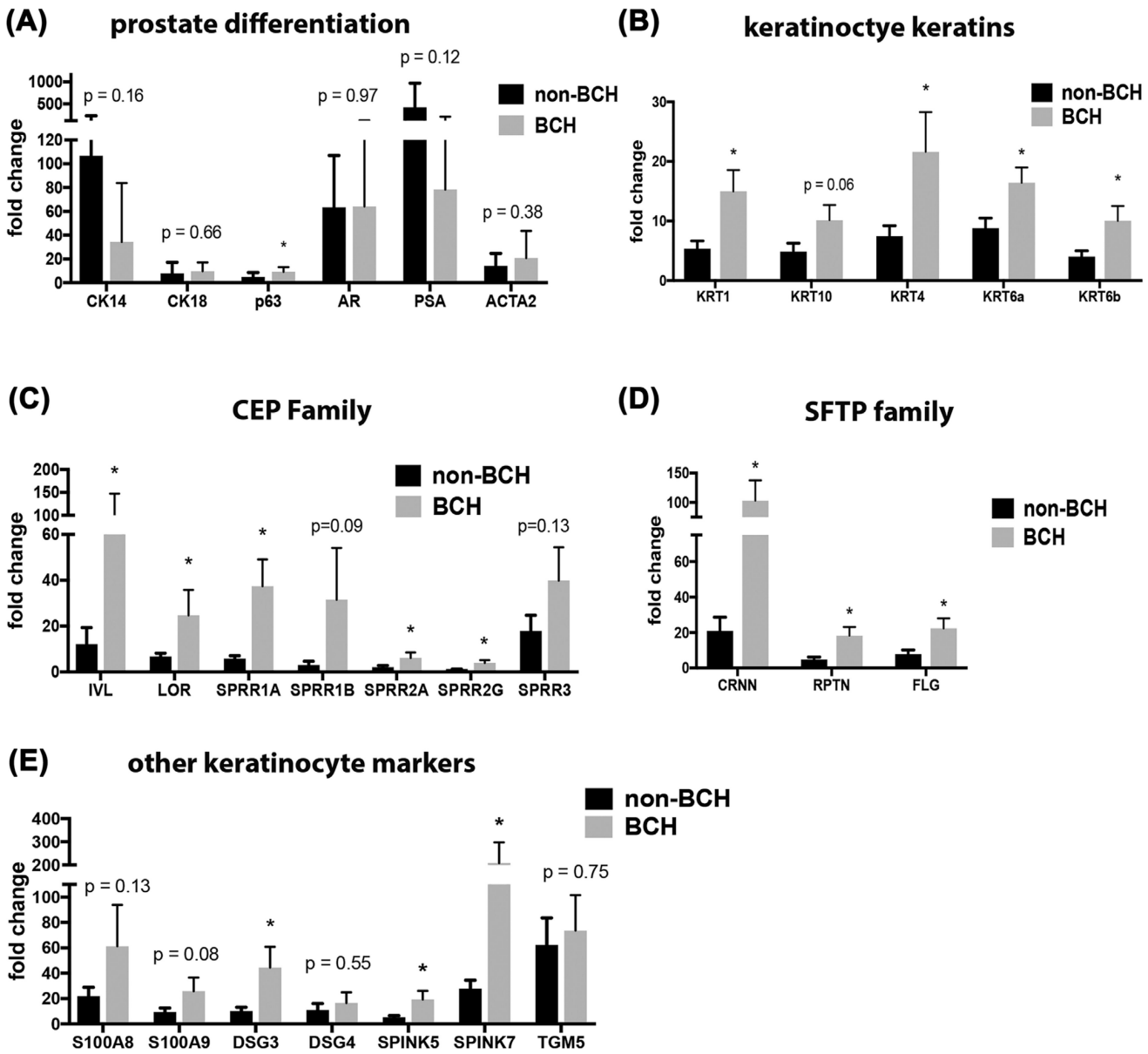

FIGURE 4.

qPCR confirmation of keratinocyte differentiation genes upregulated in BCH specimens. (A) Out of six major prostate differentiation genes analyzed, only p63 was significantly higher in BCH specimens. (B) Keratins known to be enriched in keratinocytes were significantly enriched in BCH specimens. (C) Cornified envelope protein family members were significantly enriched in BCH specimens. (D) S100 fused type protein (SFTP) family members were significantly enriched in BCH specimens. (E) An assortment of other known keratinocyte markers were increased in BCH specimens

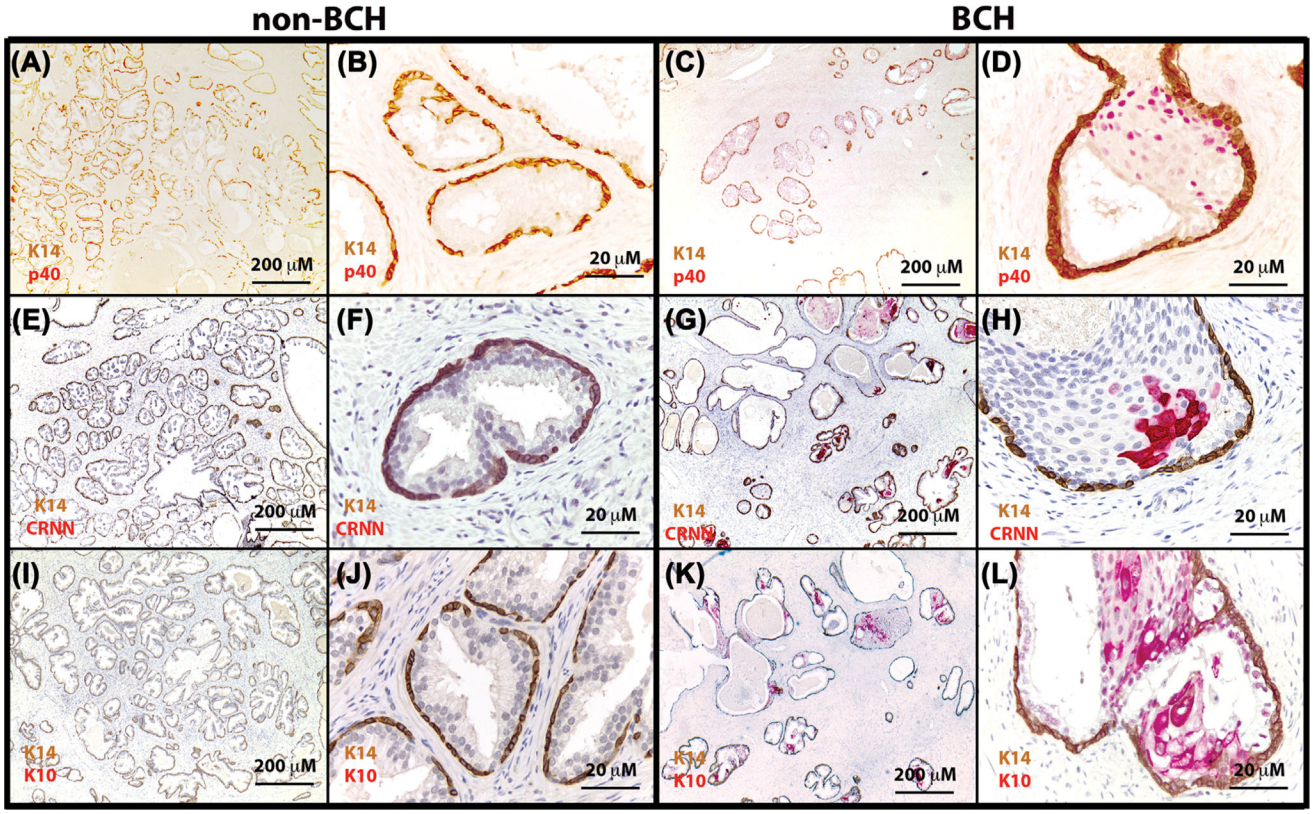

FIGURE 5.

Immunohistochemical confirmation of keratinocyte differentiation proteins. (A–D) p40 immunoreactivity was uniformly high in basal and supra-basal epithelia in BCH, but was undetectable in non-BCH specimens. No counterstain was done to enhance visualization of nuclear staining in $K14^{+}$ cells. (E-H) Cornulin (CRNN) immunoreactivity was detectable in supra-basal, $K14^{-}$ epithelia of BCH glands, but was undetectable in non-BCH glands. (I–L) Keratin 10 (K10) immunoreactivity was detectable in supra-basal, $K14^{-}$ epithelia of BCH glands, but was undetectable in non-BCH glands

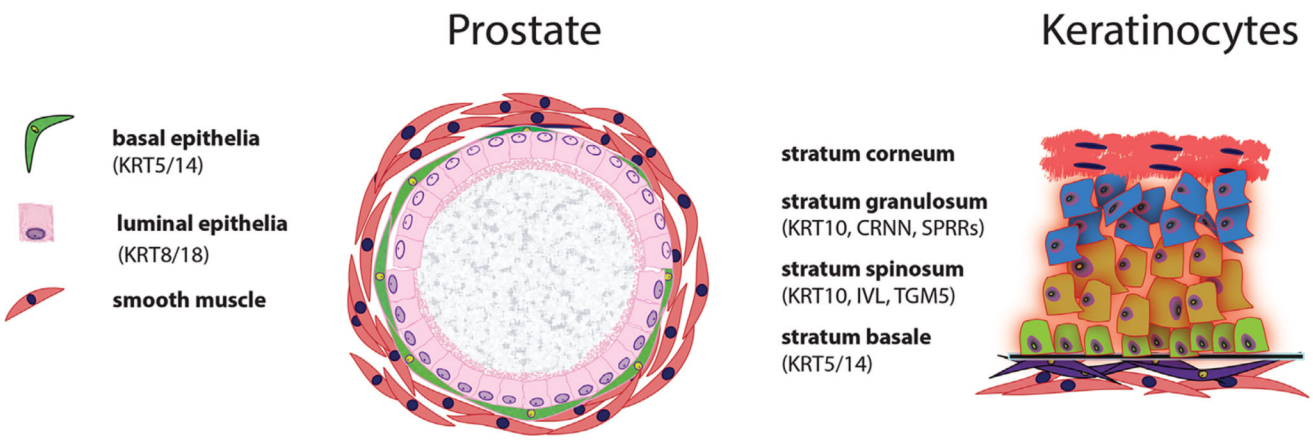

FIGURE 6.

Schematic of pseudostratified glandular epithelium in prostate versus stratified squamous epithelium of skin.

TABLE 1

Clinical characteristics of entire BPH cohort

	Age (years)	PSA (ng/mL)	Prostate volume (cc)	5ARI	Alpha blocker	Ty pe 2 diabetes	Body mass ndex
Age	1	0.103	0.307[b]	0.066	−0.104	−0.02	−0.141
Significance		0.239	0	0.44	0.22	0.812	0.098
N	141	133	134	141	141	141	140
PSA	0.103	1	0.328[b]	−0.202[a]	−0.157	0.069	−0.079
Significance	0.239		0	0.02	0.071	0.431	0.367
N	133	133	127	133	133	133	133
Prostate volume	0.307[b]	0.328[b]	1	−0.228[b]	−0.223[b]	−0.083	0.019
Significance	0	0		0.008	0.01	0.341	0.826
N	134	127	134	134	134	134	134
5ARI	0.066	−0.202[a]	−0.228[b]	1	0.346[b]	0.102	−0.018
Significance	0.44	0.02	0.008		0	0.23	0.829
N	141	133	134	141	141	141	140
Alpha blocker	−0.104	−0.157	−0.223[b]	0.346[b]	1	0.08	−0.07
Significance	0.22	0.071	0.01	0		0.346	0.409
N	141	133	134	141	141	141	140
Type 2 diabetes	−0.02	0.069	−0.083	0.102	0.08	1	0.054
Significance	0.812	0.431	0.341	0.23	0.346		0.524
N	141	133	134	141	141	141	140
Body mass index	−0.141	−0.079	0.019	−0.018	−0.07	0.054	1
Significance	0.098	0.367	0.826	0.829	0.409	0.524	
N	140	133	134	140	140	140	140

[a] less than or equal to 0.05.

[b] less than or equal to 0.01.

TABLE 2

Clinical characteristics of BCH versus non-BCH cohorts

	Non-BCH cohort	**BCH cohort**	***P* value**
Age (years), IQR	66.2, 65–68	66.5, 61–72	0.892
PSA (ng/mL), IQR	6.98, 6.02–7.94	5.14, 2.92–7.38	0.27
prostate volume (cc), IQR	120, 110–130	136, 86–187	0.385
5ARI treatment	47%	69%	0.155
Alpha blocker treatment	68%	69%	0.936
Type 2 diabetes	31%	38%	0.598
Body mass index, IQR	29.2, 28.4–29-9	27.8, 25.6–30.0	0.273
	n = 128	*n* = 13	

TABLE 3

Antibodies for IHC and FACS

IHC	**Company**	**Catalog**	**Concentration**		
CK14	Vector	vp-c410	1:500		
Ki67	Vector	vp-RM04	1:200		
AR	Santa Cruz	sc-816	1:200		
CK8/18	Fitzgerald	20R-CP004	1:500		
p63	ProteinTech	12143-1-AP	1:100		
CRNN	Sigma	HPA024343	1:200		
p40	Novus	NBP2-29467	1:1000		
CK10	Thermo Scientific	PA5-32459	1:100		
FACS	Company	Catalog	Concentration	Clone	Conjugate
CD45	Tonbo	25-0459	1:100	HI30	APC/Cy7
CD326	BIoLegend	324226	1:20	9C4	BV650
CD26	BioLegend	302704	1:20	BA5b	FITC
CD31	BD Biosciences	561653	1:20	WM59	V450
CD49f	BioLegend	313612	1:100	GoH3	PE
ghost	Tonbo	13-0863	1:1000	N/A	V450

TABLE 4

qRT-PCR primers for human genes

Gene	Forward	Reverse
KRT14	AGATCAAAGACTACAGTCCC	ACTCTGTCTCATACTTGGTG
KRT18	GGAAGTAAAAGGCCTACAAG	GTACTTGTCTAGCTCCTCTC
TP63	TCTGTTTCTGAAGTAAGTGC	TCTGTTTCTGAAGTAAGTGC
AR	GGCGGGCCAGGAAAGCGACT	TCCCTGGCAGTCTCCAAACGCAT
ACTA2	AGATCAAGATCATTGCCCC	TTCATCGTATTCCTGTTTGC
KLK3	TATGAGCCTCCTGAAGAATC	GAACTCCTCTGGTTCAATG
KRT1	GAGGATATAGCCCAGAAGAG	ATCTAAGTCTCTGGATCACAC
KRT10	AAGAGCAAGGAACTGACTAC	CGTCTCAATTCAGTAATCTCAG
KRT4	GTACAGAATGTCTGGAGAATG	TGGTAGAGATGATCTTGCTG
KRT6A	TGAGGATGAAATCAACAAGC	GAATTTGTGACTCTGAAGAAGG
KRT6B	GAATTTGTGACTCTGAAGAAGG	GGAAGTTGATCTCATCTGTAAG
IVL	TTACTGTGAGTCTGGTTGAC	TGTTCATTTGCTCCTGATG
LOR	GTTTGCAAATCCTTCATGTC	AAACCAAAGAGGCTAAACAG
SPRR1A	GTATACCAGCTTTCTGTCTC	CAAGGTTGTTTCACCTGC
SPRR1B	TATTCCTCTCTTCACACCAG	TCCTTGGTTTTGGGGATG
SPRR2A	GAGAACCTGATCCTGAGAC	AGGAGGATATTTCTGCTGG
SPRR2G	CACTGATGCTATCTTCTTGC	CTGGTAAGACATCTCTCCTC
SPRR3	GGATTCTTCAAAGAGTGTGTC	TCTTTACTCCATCGGCAG
CRNN	ACAGCTAGAGAGCTGTATTC	GAAAGACCTAAAAGGGAAGC
RPTN	ATCCTCCAGAGACCAAATG	TCTAGCTTATGATAGCAGGC
FLG	AATTTCGGCAAATCCTGAAG	CTTGAGCCAACTTGAATACC
S100A8	GTATATCAGGAAAAAGGGTGC	TACTCTTTGTGGCCTTTCTTC
S100A9	GCAAAATTTTCTCAAGAAGGAG	CCATCAGCATGATGAACTC
DSG3	ATTGGTGGATTATATCCTGGG	TATTTGACATTTGAGGCAGC
DSG4	TTGATTCAAGAACTGGTGAG	ATCATCTATAGCCAGGATCTC
SPINK5	GATTCTGAGATGTGCAAAGAC	ATCAGGTTTCATGACAGAG
SPINK7	CGAGAGCTTGAAAAGTAATGG	GAAAGAAACTCAGTCAGAGC
TGM5	ACACTCTCTCCTAAAGAAGC	GTGATGCTTGGATAAGATAAGG
RPL27	CGTCAATAAGGATGTCTTCAG	GTTCTTGCCTGTCTTGTATC